View metadata, citation and similar papers at core.ac.uk
brought to you by CORE
provided by UT Digital Repository

The Astrophysical Journal, 693:L6–L10, 2009 March 1 doi:10.1088/0004-637X/693/1/L6
© 2009. The American Astronomical Society. All rights reserved. Printed in the U.S.A.

THE PHYSICS OF CRYSTALLIZATION FROM GLOBULAR CLUSTER WHITE DWARF STARS IN NGC 6397

D. E. Winget[1,2], S. O. Kepler[2], Fabíola Campos[2], M. H. Montgomery[1,3], Leo Girardi[4], P. Bergeron[5], and Kurtis Williams[1,6]
[1] Department of Astronomy, University of Texas at Austin, Austin, TX, USA; dew@astro.as.utexas.edu
[2] Instituto de Física, Universidade Federal do Rio Grande do Sul, Porto Alegre, RS, Brazil
[3] Delaware Asteroseismic Research Center, Mt. Cuba Observatory, Greenville, DE, USA
[4] INAF-Padova Astronomical Observatory, Padova, Italy
[5] Département de Physique, Université de Montréal, C. P. 6128, Succ. Centre-Ville, Montréal, Québec H3C 3J7, Canada
Received 2008 August 18; accepted 2009 January 16; published 2009 February 11

ABSTRACT

We explore the physics of crystallization in the deep interiors of white dwarf (WD) stars using the color–magnitude diagram and luminosity function constructed from proper-motion cleaned *Hubble Space Telescope* photometry of the globular cluster NGC 6397. We demonstrate that the data are consistent with the theory of crystallization of the ions in the interior of WD stars and provide the first empirical evidence that the phase transition is first order: latent heat is released in the process of crystallization as predicted by van Horn. We outline how these data can be used to observationally constrain the value of $\Gamma \equiv E_{\rm Coulomb}/E_{\rm thermal}$ near the onset of crystallization, the central carbon/oxygen abundance, and the importance of phase separation.

Key words: dense matter – equation of state – globular clusters: individual (NGC 6397) – stars: luminosity function, mass function – white dwarfs

1. STAR FORMATION HISTORY AND PHYSICS FROM THE WHITE DWARF STARS

White dwarf (WD) stars are the inevitable progeny of nearly all ($\simeq$97%) stars (e.g., Fontaine et al. 2001, hereafter FBB). Their distribution can be used to extract two things: age of the stellar population and cooling physics of the WD stars. The two are interrelated, but qualitatively different. Extracting the age and history of star formation has become known as WD cosmochronology. An excellent review emphasizing this connection and the attendant uncertainties is given by FBB.

The techniques of WD cosmochronology have been successfully applied to the disk by a number of investigators (e.g., Winget et al. 1987; Wood 1992; Hansen & Liebert 2003, and references therein) and are being continuously refined. They have also been applied to a variety of open clusters and calibrated against main-sequence turnoff and related methods (e.g., Kalirai et al. 2007; DeGennaro et al. 2008, and references therein). The *Hubble Space Telescope* (*HST*) photometry obtained by Richer and Hansen and their collaborators (Hansen et al. 2002, 2007; Richer et al. 2008) has yielded a new harvest of information for WD populations. They have used the Advanced Camera on the *HST* to reach the terminus of the WD cooling sequence, giving us a qualitatively different tool for analyzing the WD population. Hansen et al. (2007) used Monte Carlo techniques in conjunction with their cooling models to determine the age of NGC 6397 from the WD stars, attempting to account for uncertainties in the basic physical parameters of the WD stars to determine an age for the cluster; using goodness-of-fit criteria, they arrive at an age for the cluster, based on WD cooling, of 11.47 ± 0.47 Gyr.

Finding the signature of the key physical properties of the WD stars in the disk luminosity function (hereafter LF) has proven more difficult than getting an age constraint. This is because the disk population contains stars formed at different times and from different main-sequence progenitors. This is greatly simplified in a cluster sample and, most of all, in an old globular cluster. In this Letter, we focus on the *HST* photometry of NGC 6397 and the distribution of WD stars in the color–magnitude diagram (hereafter CMD). We report evidence for a "bump" in the LF due to the release of the latent heat of crystallization and we show how this can be refined to yield more accurate measures of these processes.

2. ANCHORING THE WD EVOLUTIONARY SEQUENCES IN THE COLOR–MAGNITUDE PLANE

We fit main-sequence, pre-WD, and WD evolutionary models simultaneously. The main-sequence and pre-WD models we used for this work were computed with the Padova stellar evolution code (Marigo et al. 2008). We used a variety of metallicities to determine the best fit to the main-sequence and WD models.

Our WD evolutionary models have updated constitutive physics (see, e.g., Bischoff-Kim et al. 2008). We place the new generation of WD evolutionary models of DA and DB WD stars in the observed F_{814W} versus F_{606W} CMD using P. Bergeron's model atmosphere grids[7] (for a detailed description, see Bergeron et al. 1995; Holberg & Bergeron 2006; Holberg et al. 2008) along with an analytical correction to the Kowalski (2007) results for the effect of Lyα far red-wing absorption. This correction is small and will be discussed in a forthcoming paper.

Our best fit of the CMD in the natural ACS color system gives a metallicity of $Z = 0.00012 \pm 0.00001$, $E(F_{606W} - F_{814W}) = 0.22 \pm 0.02$, and $(m - M) = 12.49 \pm 0.05$ (Figure 1) and a main-sequence turnoff age of $12^{+0.5}_{-1.0}$ Gyr. The age is consistent with the values found by Richer et al. (2008) and Hansen et al. (2007), even though they used the Dartmouth Evolutionary Sequence (DES). The metallicity is a factor of two lower than Richer et al. (2008) but is in agreement with the independent direct spectroscopic determinations based on VLT data (Korn et al. 2007). The values of these parameters fix the WD cooling tracks

[6] NSF Astronomy & Astrophysics Postdoctoral Fellow.

[7] http://www.astro.umontreal.ca/~bergeron/CoolingModels/.

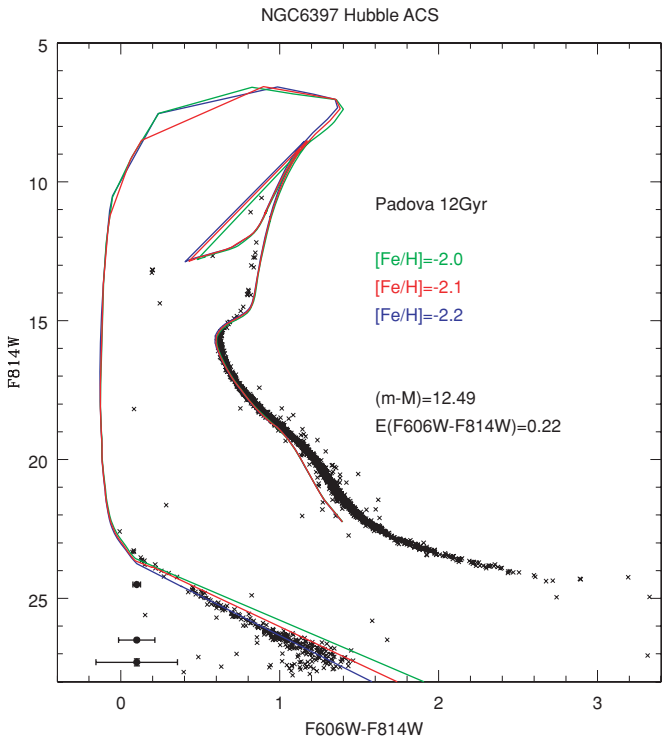

Figure 1. Best fit to the proper-motion screened *HST* data on NGC 6397 using the Padova stellar evolution code (Marigo et al. 2008). This fit gives [Fe/H] $= -2.2$, $(m - M) = 12.49$, and $E(F_{606W} - F_{814W}) = 0.22$. This anchors our WD sequences in the CMD.

in the CMD and eliminate the freedom to slide the tracks as has been done in other works (e.g., Hansen et al. 2007). This constrains the best-fit total WD mass throughout the CMD. It is clear from Figure 2 that the tracks fit the bulk of the sample well.

The data (see Figure 2) are taken from the proper-motion selected sample of Richer et al. (2008). This is a more homogeneous sample than that of Hansen et al. (2007) but is smaller because of the reduced area and magnitude limits of the proper-motion data. Four features stand out in Figure 2: there is a gap in the distribution near $F_{814W} = 24.5$ that may be statistically significant, there is a noticeable concentration of stars near $F_{814W} = 26.5$, there is a terminus at approximately $F_{814W} = 27.6$, and a noticeable turn to the blue before the terminus. These last two features were noted in Hansen et al. (2007). In this Letter, we focus on what we can learn from the concentration, or clump, of stars near 26.5, providing a physical explanation.

3. PHYSICS WITH THE CMD AND LF

The CMD constrains the mechanical and thermal properties of the WD stars (Richer et al. 2008). Once the evolutionary tracks have been anchored by the main sequence and WD sequence simultaneously as described above, we can move on to exploring the physics contained in the CMD. Hansen et al. (2007) point out that the location of the terminus provides a simple lower limit to the age of the cluster from the WD cooling times. For our models, this WD cooling limit is reached at about 10.5 Gyr for pure carbon core models. This age limit is consistent with the values quoted in Hansen et al. (2007) and Richer et al. (2008). The position of the tracks is insensitive to processes affecting only the age; to examine these we must look to the LF, the number of stars observed as a function of magnitude.

For the parameters described above, it is evident from Figure 2 that models with masses in the range of 0.500–0.535 $M_{\odot}$ best fit the region near the center of the clump. This increases slightly for decreased values of $m - M$ and is also a function of the reddening. We emphasize again that simultaneously fitting the main sequence and WD sequence provides tight constraints on both the distance modulus and the reddening.

In Figure 3, we show the LF of both the Hansen et al. (2007) and Richer et al. (2008) samples. The peak in both LFs near $F_{814W} = 26.5$ suggests that evolution slows through this region. In the sample of Hansen et al. (2007), the LF continued to rise well past this peak, so it was not the maximum of the distribution; it completely dominates the distribution after the application of the proper-motion selection (Richer et al. 2008). The completeness estimates of both samples have been carefully considered by the respective authors (Figure 3, dotted lines) and the relatively slow variation of the completeness near this peak implies it is not the result of incompleteness. We therefore seek a physical explanation of this peak in the context of a physical process that occurs near this point in the models.

Two processes occur in the dominant DA models near this point: crystallization and convective coupling (e.g., FBB). Crystallization, through the release of latent heat, slows down evolution and produces a bump in the LF. Convection, when it reaches down to the degeneracy boundary, decreases the insulation of the nondegenerate envelope and temporarily increases the total temperature gradient; this serves to slow down the evolution, briefly, then causes it to speed up again. This produces a broad feature in the WD cooling curve that will have a signature in the LF.

3.1. The Γ of Crystallization

Crystallization in the dense Coulomb plasma of WD interiors was theoretically predicted independently by Kirzhnits (1960), Abrikosov (1960), and Salpeter (1961) to occur when the ratio of the Coulomb energy to the thermal energy of the ions (the ratio "Γ") is large. For a one-component plasma (OCP), there is universal agreement among different theoretical approaches that crystallization occurs when $\Gamma \simeq 175$ (e.g., Slattery et al. 1982; Stringfellow et al. 1990; Potekhin & Chabrier 2000; Horowitz et al. 2007). There is a similar consensus, based largely on a density-functional approach, that this value of Γ also holds for a binary carbon and oxygen mixture. Such a mixture is likely relevant to WD interiors. Recently, Horowitz et al. (2007) used a massive molecular dynamics computation to explore crystallization in a dense Coulomb plasma. They found $\Gamma = 175$ for an OCP, while for a specific mixture of elements they found $\Gamma \simeq 237$. As we show, such a difference is potentially measurable from the observations of WD stars in globular clusters or older open clusters.

3.2. LFs with and without Crystallization

Hansen et al. (2007) demonstrated in their analysis that the entire observed sequence represents a very narrow range of WD masses, including magnitudes well below $F_{814W} = 26.5$. It is therefore reasonable for purposes of this initial exploration to adopt a fiducial mass. On the basis of the model tracks in the CMD shown in Figure 2, we choose the model that passes nearest the color of the red edge of the clump of stars corresponding to the peak in the LF; this model has a mass of 0.5 $M_{\odot}$. For the layer masses, we assume $M_{\rm H}/M_{\star} = 10^{-4}$ and $M_{\rm He}/M_{\star} = 10^{-2}$ for the DA sequences, and $M_{\rm He}/M_{\star} = 10^{-2}$

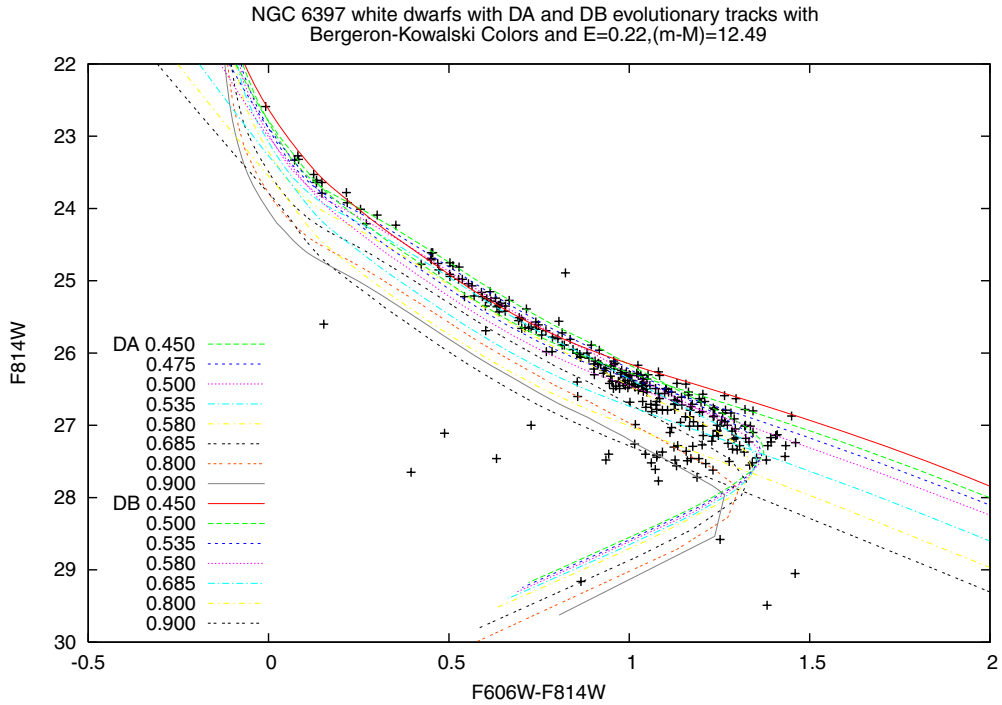

Figure 2. NGC 6397 WDs with DA and DB evolutionary sequences using the atmospheres of Holberg & Bergeron (2006). This includes an analytical adjustment for the effects of Lyα red-wing opacity as computed by Kawalski (2007).

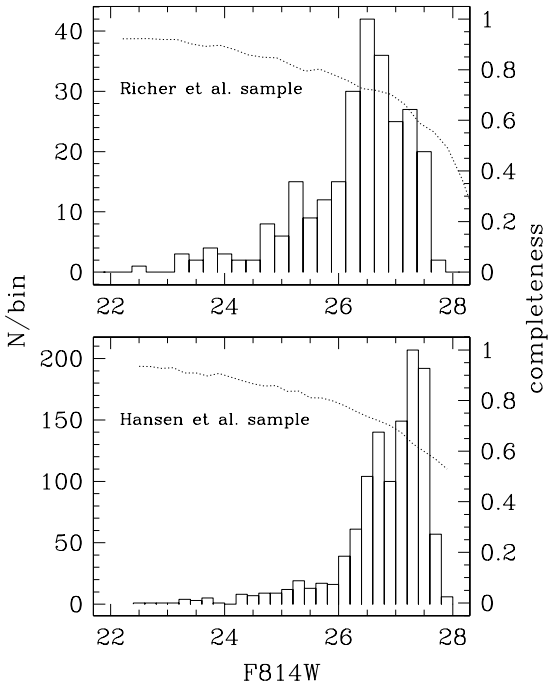

Figure 3. Top panel: the observed WD LF (histogram) and completeness relation (dotted line) of the Richer et al. (2008) sample for NGC 6397. Lower panel: the same for the Hansen et al. (2007) sample. For both samples, we note that the completeness changes fairly slowly over the region of the observed rapid falloff of stars while remaining above 50%.

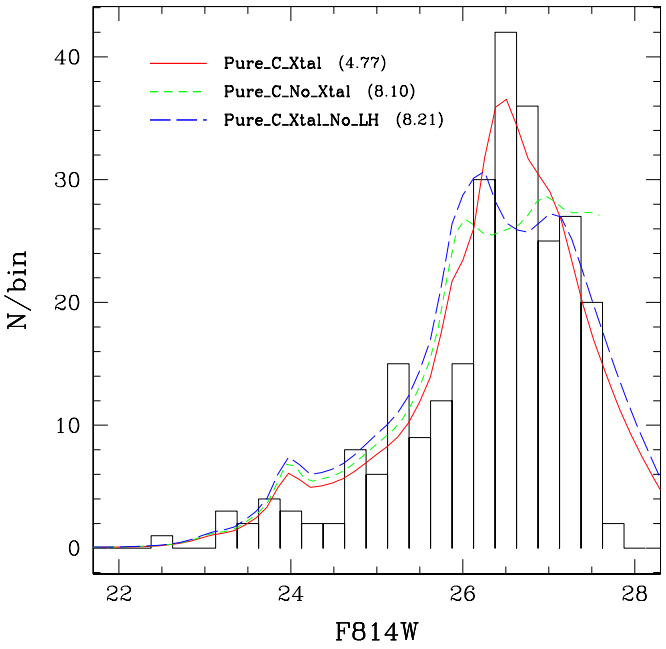

Figure 4. Observed WD LF of NGC 6397 (Richer et al. 2008, histogram) with LFs from theoretical evolutionary sequences of 0.5 $M_{\odot}$ DA models with pure carbon cores (lines): crystallization with (Pure_C_Xtal) and without (Pure_C_Xtal_No_LH) the release of latent heat, and excluding the physics of crystallization altogether (Pure_C_No_Xtal). The normalization of the theoretical curves is chosen to minimize the rms residuals in the neighborhood of the peak, between the magnitudes of 25.1 and 27.7, the faintest value calculated for the no crystallization case. The value of the average residual for each curve is listed in the legend, e.g., it is 4.77 for the "Pure_C_Xtal" case.

for the DB sequence. We adopt a carbon core model including the effects of crystallization for this sequence.

Assuming a constant star formation rate, the theoretical LF is proportional to the "cooling function" of an evolutionary model sequence. This function is given by the derivative (dt/dm), where m is the F_{814W} magnitude of a given model and t is its age. Since we will be comparing directly with the data, we also multiply the theoretical LF by the completeness correction given explicitly in Table 4 of Richer et al. (2008) and shown in the top panel of our Figure 3. Finally, we normalize the resulting

curves by minimizing their rms residuals in the neighborhood of the peak, between an F_{814W} of 25.1 and 27.5.

In Figure 4, we show the LF of our fiducial sequence (Pure_C_Xtal), that of a sequence with crystallization artificially suppressed (Pure_C_No_Xtal), and that of one including crystallization but artificially excluding the latent heat of crystallization (Pure_C_Xtal_No_LH); all are plotted over a histogram of the observed LF. The no crystallization and no latent heat sequences show evidence of a bump due to convective coupling around $F_{814W} \sim 26$, but do not continue to rise through the observed maximum; this is clearly inconsistent with the data, and no adjustment of mass or internal composition can bring them into good agreement. In terms of χ^2, for average observational errors of ~5.5 stars/bin in the neighborhood of the peak, we have $\chi^2 = 0.75$ for the crystallizing sequence and $\chi^2 \sim 2.2$ for the no crystallization and no latent heat sequences, a nearly threefold increase in χ^2. Thus, the sequence with crystallization provides a much better match to the data.

3.3. Constraining Crystallization, Phase Separation, and Core Composition

In the years since van Horn (1968), the realization that the cores of normal mass WD stars should consist of a mixture of carbon and oxygen implied that crystallization may also release energy resulting from phase separation of the carbon and oxygen (Stevenson 1977; Barrat et al. 1988; Segretain & Chabrier 1993; Segretain et al. 1994; Isern et al. 2000). This occurs because when a carbon/oxygen mixture crystallizes, the oxygen content of the solid should be enhanced. Since WDs crystallize from the center outward, this leads to a net transport of oxygen inward and carbon outward, and because oxygen is slightly heavier than carbon this differentiation releases gravitational energy.

We have included this energy in our models as described in Montgomery et al. (1999). For these computations, we have assumed the carbon and oxygen abundances are equal throughout the core. This underestimates the oxygen abundance compared to that predicted by standard stellar evolution calculations (e.g., Salaris et al. 1997), but the remaining uncertainty in the C(α, γ)O reaction rate (Metcalfe et al. 2002; Assunção et al. 2006) leads to a degree of uncertainty in the C/O ratio and profile. In Figure 5, we show several LFs: crystallization only (CO_Xtal), crystallization with phase separation (CO_Xtal_PS), no crystallization (CO_No_Xtal), pure oxygen core with crystallization (Pure_O_Xtal), and a pure carbon DB sequence (Pure_C_DB_Xtal). As is readily apparent, all of these sequences have a peak which is too bright by at least 0.5 mag in F_{814W}.

These results have several interesting possible interpretations. First, the results seem to suggest that the oxygen content of these stars is relatively small or zero, since it is the higher crystallization temperature of oxygen which shifts the peak in the LF to smaller magnitudes. The only way to accommodate more oxygen would be to have lower-mass models, in conflict with the distance modulus (Hansen et al. 2007). The colors (e.g., Figure 2) also make it difficult to appeal to lower masses with higher oxygen abundances. Additionally, for plausible initial–final mass relations (IFMRs), the main-sequence lifetime for single stars becomes more problematic with lower WD masses even with the IFMR dependency on metallicity of Meng et al. (2008). Thus, the constraint on the interior oxygen abundance becomes stronger. Taken at face value, these results indicate that the carbon-to-oxygen ratio is much greater than 1, and we will

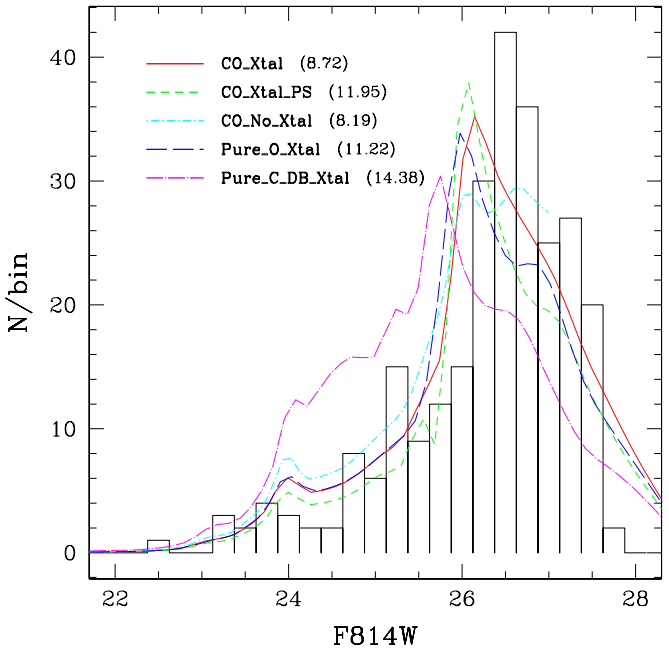

Figure 5. Same as Figure 4 but for DA model sequences with uniform, 50:50 carbon/oxygen cores: crystallization only (CO_Xtal), crystallization *and* phase separation (CO_Xtal_PS), and no crystallization (CO_No_Xtal). In addition, we show a pure oxygen DA sequence (pure_O_Xtal) and a pure carbon DB sequence (pure_C_DB_Xtal). All models have 0.5 $M_\odot$.

be able to make a more quantitative statement from our future more complete Bayesian statistical analysis (DeGennaro et al. 2009, in preparation).

Second, as shown in Figure 4, the data are consistent and well fitted by carbon core models *with* crystallization and the release of latent heat, but not by models without. This confirms the prediction of van Horn (1968) that crystallization is a first-order phase transition and releases the latent heat of crystallization. Were it not so, crystallization would leave no sharp peak at this magnitude in the observed LF. This impacts our understanding of solid-state physics at extremely high density: it is the first empirical confirmation of the release of latent heat during crystallization—an important theory that has a large impact on WD ages, as has been pointed out by van Horn (1968) and many authors in the intervening years.

Third, it is possible a priori that a significant fraction of the observed WDs may be DBs. The mismatch of observed LF and the DB sequence in Figure 5 essentially eliminates pure He atmosphere as a significant component of the sample (as shown by Hansen et al. 2007), but not models that become mixed (H/He) as they cool; we explore this possibility in a forthcoming paper.

Fourth, the "best-fit" fiducial sequence in Figure 4 begins crystallizing near the value of $\Gamma_{\rm xtal} \equiv E_{\rm Coulomb}/E_{\rm thermal} \sim 170$. If the actual value is higher (lower), then crystallization will occur at lower (higher) luminosities. Higher values allow fits with larger amounts of oxygen in their cores. In addition, Potekhin & Chabrier (2000) show that even for a pure composition theoretical uncertainties in the polarization of the electron Fermi gas and quantum effects in the liquid and solid phase can alter the value of $\Gamma_{\rm xtal}$. In future analyses, an accurate determination of the mass, distance, and reddening will lead to an accurate determination of $\Gamma_{\rm xtal}$ and the core composition.

Finally, we note that the central density and temperature associated with a particular value of F_{814W} through the model

atmospheres is sensitive only to the mass–radius relationship set by the degenerate electron pressure support. This is very insensitive to the C/O relative abundances—these produce differences of $\delta F_{814W} < 0.05$. This implies that the value of Γ in the center, at the peak of the LF for example, is sensitive only to the interior composition. Therefore, we conclude that the onset of crystallization is determined by the particular mixture and the value of Γ for that mixture. Comparison of the theoretical models and the data promises to provide important measures of the onset and development of crystallization.

4. DISCUSSION, SUMMARY, AND FUTURES OF EXPLORING WD PHYSICS WITH CMDS

Although we are not focused on uncertainties, it is reasonable to examine how changing the distance modulus might affect the results. Put another way, how much does the distance have to change to reproduce the peak of the observed LF with oxygen crystallization rather than carbon? The answer is contained in Figure 5. Here we see that to make the location of the peak of the LF consistent with oxygen crystallization we have to lower the distance modulus by a little more than 0.5 mag—this possibility is excluded by the main-sequence fitting (Richer et al. 2008).

We have shown that simultaneously fitting the main sequence and the WDs in a cluster gives the best possible constraint on distance, metallicity, and reddening corrections. Physically realistic atmosphere calculations then allow us to place evolutionary tracks in the CMD. The number distribution of stars contains important information on the internal physics of the WD stars. This allows us to explore the physics of crystallization. We present evidence that the data are most consistent with a first-order phase transition, releasing latent heat during crystallization, as proposed by van Horn (1968). The current data place constraints on the onset of crystallization, the central carbon/oxygen abundance, and the composition of the envelope at the degeneracy boundary. We will improve these constraints with a more complete Bayesian statistical analysis in the near future. This work also points to the importance of forthcoming data on additional clusters as well as increasing the sample of stars through more *HST* fields on this cluster. This work also underscores the essential nature of more proper-motion data to get the most information out of these kinds of studies.

Pulsations may also allow an asteroseismological determination of the crystallized mass fraction for massive pulsators, as shown by Metcalfe et al. (2004) for the DAV BPM 37093, although this claim has been challenged by Brassard & Fontaine (2005). While certainly important, we note that asteroseismological analyses do not probe the latent heat of crystallization; this quantity is accessible only through the WD LF, as demonstrated in this Letter. To this end, we eagerly anticipate the forthcoming *HST* observations of this cluster. These will provide a proper-motion screened sample over a larger area of the cluster and to fainter magnitudes, providing an exacting test of the ideas put forth in this Letter.

The authors thank A. Zabot for help computing the isochrones, Ted von Hippel and Hugh van Horn for useful discussions, and Brad Hansen and referees for suggesting improvements. D.E.W., S.O.K., and F.C. are fellows of CNPq-Brazil. M.H.M. and K.A.W. are grateful for the financial support of the National Science Foundation under awards AST-0507639 and AST-0602288, respectively, and M.H.M. acknowledges the support of the Delaware Asteroseismic Research Center. This work was supported in part by the NSERC Canada and by the Fund FQRNT (Québec). P.B. is a Cottrell Scholar of Research Corporation.

REFERENCES

Abrikosov, A. A. 1960, Zh. Eksp. Teor. Fiz., 39, 1798
Assunção, M., et al. 2006, Phys. Rev. C, 73, 055801
Barrat, J. L., Hansen, J. P., & Mochkovitch, R. 1988, A&A, 199, L15
Bergeron, P., Wesemael, F., Lamontagne, R., Fontaine, G., Saffer, R. A., & Allard, N. F. 1995, ApJ, 449, 258
Bischoff-Kim, A., Montgomery, M. H., & Winget, D. E. 2008, ApJ, 675, 1505
Brassard, P., & Fontaine, G. 2005, ApJ, 622, 572
DeGennaro, S., von Hippel, T., Winget, D. E., Kepler, S. O., Nitta, A., Koester, D., & Althaus, L. 2008, AJ, 135, 1
Fontaine, G., Brassard, P., & Bergeron, P. 2001, PASP, 113, 409
Hansen, B. M. S., & Liebert, J. 2003, ARA&A, 41, 465
Hansen, B. M. S., et al. 2002, ApJ, 574, L155
Hansen, B. M. S., et al. 2007, ApJ, 671, 380
Holberg, J. B., & Bergeron, P. 2006, AJ, 132, 1221
Holberg, J. B., Bergeron, P., & Gianninas, A. 2008, AJ, 135, 1239
Horowitz, C. J., Berry, D. K., & Brown, E. F. 2007, Phys. Rev. E, 75, 066101
Isern, J., García-Berro, E., Hernanz, M., & Chabrier, G. 2000, ApJ, 528, 397
Kalirai, J. S., Bergeron, P., Hansen, B. M. S., Kelson, D. D., Reitzel, D. B., Rich, R. M., & Richer, H. B. 2007, ApJ, 671, 748
Kirzhnits, D. A. 1960, Sov. Phys.—JETP, 11, 365
Korn, A. J., Grundahl, F., Richard, O., Mashonkina, L., Barklem, P. S., Collet, R., Gustafsson, B., & Piskunov, N. 2007, ApJ, 671, 402
Kowalski, P. M. 2007, A&A, 474, 491
Marigo, P., Girardi, L., Bressan, A., Groenewegen, M. A. T., Silva, L., & Granato, G. L. 2008, A&A, 482, 883
Meng, X., Chen, X., & Han, Z. 2008, A&A, 487, 625
Metcalfe, T. S., Montgomery, M. H., & Kanaan, A. 2004, ApJ, 605, L133
Metcalfe, T. S., Salaris, M., & Winget, D. E. 2002, ApJ, 573, 803
Montgomery, M. H., Klumpe, E. W., Winget, D. E., & Wood, M. A. 1999, ApJ, 525, 482
Potekhin, A. Y., & Chabrier, G. 2000, Phys. Rev. E, 62, 8554
Richer, H. B., et al. 2008, AJ, 135, 2141
Salaris, M., Dominguez, I., Garcia-Berro, E., Hernanz, M., Isern, J., & Mochkovitch, R. 1997, ApJ, 486, 413
Salpeter, E. E. 1961, ApJ, 134, 669
Segretain, L., & Chabrier, G. 1993, A&A, 271, L13
Segretain, L., Chabrier, G., Hernanz, M., García-Berro, E., Isern, J., & Mochkovitch, R. 1994, ApJ, 434, 641
Slattery, W. L., Doolen, G. D., & Dewitt, H. E. 1982, Phys. Rev. A, 26, 2255
Stevenson, D. J. 1977, PASA, 3, 167
Stringfellow, G. S., Dewitt, H. E., & Slattery, W. L. 1990, Phys. Rev. A, 41, 1105
van Horn, H. M. 1968, ApJ, 151, 227
Winget, D. E., Hansen, C. J., Liebert, J., van Horn, H. M., Fontaine, G., Nather, R. E., Kepler, S. O., & Lamb, D. Q. 1987, ApJ, 315, L77
Wood, M. A. 1992, ApJ, 386, 539